Catalysis Today 175 (2011) 528–533

Contents lists available at ScienceDirect

Catalysis Today

journal homepage: www.elsevier.com/locate/cattod

Impact of sorbitol addition on the structure and performance of silica-supported cobalt catalysts for Fischer–Tropsch synthesis

Jingping Hong[a,b], Eric Marceau[b,c,*], Andrei Y. Khodakov[a,c,**], Anne Griboval-Constant[a], Camille La Fontaine[d], Françoise Villain[d], Valérie Briois[c,d], Petr A. Chernavskii[e]

[a] Unité de Catalyse et de Chimie du Solide, UMR 8181 CNRS, Bât. C3, Université Lille 1-ENSCL-Ecole Centrale de Lille, 59655 Villeneuve d'Ascq, France
[b] Laboratoire de Réactivité de Surface, UMR 7197 CNRS, UPMC, 75005 Paris, France
[c] CNRS, France
[d] Synchrotron SOLEIL, L'Orme des Merisiers, BP48, Saint-Aubin, 91192 Gif-sur Yvette, France
[e] Department of Chemistry, Moscow State University, 119992 Moscow, Russia

ARTICLE INFO

Article history:
Received 15 October 2010
Received in revised form 18 February 2011
Accepted 1 March 2011
Available online 3 April 2011

Keywords:
Fischer–Tropsch synthesis
Quick-XAS
Sorbitol
Cobalt catalysts
Silica

ABSTRACT

The paper focuses on the impact of sorbitol addition on the genesis of cobalt active phases in silica-supported catalysts and on their performance in Fischer–Tropsch synthesis. The catalysts were characterized by *ex situ* and *in situ* diffuse reflectance spectroscopy in the ultraviolet and visible regions, differential thermal and thermogravimetric analyses combined with mass spectroscopy, *in situ* Quick-X-ray absorption, X-ray diffraction, H_2-temperature programmed reduction, *in situ* magnetic measurements and propene chemisorption. Sorbitol retards the decomposition of cobalt ionic complexes into Co_3O_4 during thermal treatment in air, leading to higher cobalt oxide dispersion. The smaller cobalt oxide particles in sorbitol-derived samples exhibit a much lower reducibility than those prepared without the additive. Fischer–Tropsch reaction rate is proportional to the number of cobalt metal sites, which is a function of both cobalt dispersion and cobalt reducibility. It depends in a complex manner on the initial sorbitol content.

1. Introduction

Due to the increasing demands of environmental friendly liquid fuels, the Fischer–Tropsch (FT) synthesis, which converts coal-based, biomass-based and/or natural gas-derived syngas into clean hydrocarbons fuels with high cetane numbers and low contents of sulfur and aromatics [1–3], has gained significant attention in recent years.

Cobalt-based catalysts are widely used in low temperature Fischer–Tropsch process to produce long-chain hydrocarbons. They are usually supported by refractory oxides (SiO_2, Al_2O_3, etc.). Cobalt catalysts have many advantages, such as high activity, high selectivity to linear hydrocarbons and low activity for the water–gas shift reaction. Supported cobalt catalysts for FT synthesis are commonly prepared by aqueous impregnation with cobalt nitrate or co-impregnation with promoters or additives. This step is followed by thermal treatments in air and reduction in hydrogen [4–7]. Fischer–Tropsch reaction proceeds on cobalt metal sites situated on the surface of reduced metal particles. Dispersion and degree of reduction are thus two primary parameters affecting the number of active cobalt sites and the catalytic activity in FT synthesis. Cobalt being 1000 times more expensive than iron, an optimization in terms of cobalt loading, dispersion and catalytic performance is necessary from the practical point of view.

Culross and Mauldin [8–10] found that addition of different chelating molecules during catalyst impregnation could influence cobalt dispersion and overall number of active cobalt metal sites in the catalysts after reduction. Our previous study also showed that the addition of sucrose during impregnation greatly enhanced cobalt dispersion [11] and resulted in a better catalytic performance in FT synthesis. Previous report [12] also suggests that impregnation of silica with mixed cobalt nitrate and cobalt acetate solutions could enhance cobalt dispersion and catalytic performance in FT synthesis. The formation of smaller oxide clusters was attributed to strong interactions between the support and cobalt precursors. The mechanism of this interaction and genesis of active phase in the catalysts prepared with addition of organic molecules is however still unclear and requires further investigation.

This work focuses on the effect of sorbitol addition on the genesis of cobalt active phase in silica-supported catalysts and on

* Corresponding author at: Laboratoire de Réactivité de Surface, UMR 7197 CNRS, UPMC, 75005 Paris, France. Tel.: +33 1 44 27 60 04; fax: +33 1 44 27 60 33.
** Corresponding author at: Unité de Catalyse et de Chimie du Solide, UMR 8181 CNRS, Bât. C3, Université Lille 1-ENSCL-Ecole Centrale de Lille, 59655 Villeneuve d'Ascq, France. Tel.: +33 3 20 33 54 39; fax: +33 3 20 43 65 61.
E-mail addresses: eric.marceau@upmc.fr (E. Marceau), andrei.khodakov@univ-lille1.fr (A.Y. Khodakov).

0920-5861/$ – see front matter © 2011 Elsevier B.V. All rights reserved.
doi:10.1016/j.cattod.2011.03.007

Table 1
Preparation and chemical composition of silica-supported cobalt catalysts.

Catalyst	Co/sorbitol molar ratio	Co content (wt.%)	Co_3O_4 particle size (nm) (XRD)	
			(3 1 1)	(4 4 0)
Co-Sorb(2)/SiO_2	2	10	4.2	–
Co-Sorb(5)/SiO_2	5	10	4.4	4.7
Co-Sorb(10)/SiO_2	10	10	6.3	6.9
Co/SiO_2	–	10	10.9	9.8

their catalytic performance in FT synthesis. Various characterization methods, such as *in situ* Quick-X-ray absorption spectroscopy, *in situ ex situ* and *in situ* diffuse reflectance spectroscopy in the ultraviolet and visible regions, TG-DTA/MS, temperature programmed reduction, *in situ* magnetic measurements and propene chemisorption were used to provide in-depth information about the way in which different amounts of sorbitol would influence the catalyst structure and ultimately the FT catalytic activity and hydrocarbon selectivity.

2. Experimental

2.1. Catalyst preparation

Cobalt-based catalysts were prepared by incipient wetness impregnation method. Commercial silica (CARiACT Q-10, 75–150 μm, S_{BET} = 300 m^2/g, TPV = 1.33 cm^3/g, pore diameter = 7.3 nm) was used as support, and the precursor of cobalt was cobalt(II) nitrate hexahydrate. The organic additive (sorbitol, $HOCH_2(CHOH)_4CH_2OH$) was introduced by co-impregnation. The samples were then dried in air at room temperature overnight and calcined in an air flow (~100 cm^3/min) up to 400 °C with a heating ramp of 2 °C/min from RT to 250 °C, and 5 °C/min from 250 °C to 400 °C. Before catalytic tests, the catalysts were reduced in H_2 flow (~40 cm^3/min g_{cat}) at 400 °C for 5 h with a ramping rate of 3 °C/min. The chemical composition of catalysts is presented in Table 1. Catalysts are labeled as Co/SiO_2 and Co-Sorb(x)/SiO_2, where "Sorb" indicates sorbitol addition and "x" corresponds to the Co/sorbitol molar ratio. Larger "x" values thus mean lower sorbitol contents in the impregnated samples. The nominal loading of cobalt in all these samples was 10 wt.%.

2.2. Catalyst characterization

Ex situ and *in situ* UV–visible (UV–vis) spectra of the catalysts were recorded in the diffuse reflectance mode on a Cary 5000 spectrometer (Varian, resolution, 1 nm) equipped with an integration sphere, a praying mantis device and a Harrick environmental cell using Teflon as reference. The heating rate and gas flows were similar to those used for calcination of the catalysts.

Combined differential thermal and thermogravimetric analyses together with mass spectrometry (DT-TGA/MS) were obtained on a TA Instruments Q600 SDT station equipped with a Pfeiffer Thermostar mass spectrometer, with the same heating procedure as catalysts calcination.

Co K-edge Quick-X-ray absorption spectra (XANES and EXAFS) were obtained in situ in transmission mode during oxidative pretreatments on the SAMBA beamline at SOLEIL (Gif-sur-Yvette, France). A Quick-EXAFS monochromator with Si(1 1 1) channel-cut was used. The oscillation frequency was 1 Hz, taking 500 ms to obtain one spectrum. The energy was scanned from 7550 to 8725 eV with incremental steps of 2 eV/point from 7550 to 7685 eV, 0.3 eV/point from 7685 to 7740 eV and 2 eV/point from 7740 to 8725 eV. The energy was calibrated to the first inflection point of a Co metal foil. XANES spectra were background corrected and normalized in the middle of the first EXAFS oscillation with the Athena package [13]. Fourier transforms (without phase correction) were calculated on $w(k)k^3\chi(k)$, where $w(k)$ is a Hanning window with a smoothness parameter equal to 1. The k limits were 2 and 11.5 $Å^{-1}$.

X-ray diffraction (XRD) patterns were recorded at room temperature on a Siemens D5000 diffractometer using Cu Kα radiation (λ = 0.15418 nm). Scans were recorded in the 2θ range between 20° and 70° using a step size of 0.02° and a step time of 5 s. The average size of Co_3O_4 particles was calculated according to the Scherrer equation [14] using the (3 1 1) and (4 4 0) XRD reflections.

The temperature programmed reduction (TPR) profiles were obtained by passing 5% H_2/Ar gas mixture through the catalyst while increasing the temperature at a linear rate using a Micromeritics Autochem II Automated Catalyst Characterization System. The sample amount for the experiments was about 50 mg. The gas flow velocity was 30 cm^3/min with a temperature ramping rate of 3 °C/min.

In situ magnetic measurements were performed using a Foner vibrating-sample magnetometer as described previously [15,16]. The experiments were conducted by passing pure H_2 through the catalyst while increasing the temperature at a linear rate. The sample amount for all measurements was around 20 mg. The temperature increased with ramping rate of 8 °C/min. The appearance of metallic cobalt species in the samples was monitored in situ by a continuous increase in sample magnetization during the reduction [15,16].

The number of surface metal sites in the catalysts was evaluated by propene chemisorption in a pulse reactor [17]. After reduction in pure hydrogen at 400 °C for 5 h, the catalyst sample (0.2 g) was cooled down to 50 °C and purged with He for several hours. Pulses of propene (0.25 cm^3) were introduced into a flow of He. The relative number of metal surface sites was estimated from the amount of chemisorbed propene.

2.3. Fischer–Tropsch synthesis

The FT synthesis reaction was carried out in a fixed-bed stainless-steel tubular micro-reactor (d_{int} = 8 mm) operating at atmospheric pressure with a H_2/CO molar ratio of 2. The catalyst loading was typically 0.5 g. Before reaction, the samples were reduced in hydrogen flow at 400 °C for 5 h, same as the reduction procedure in propene chemisorption. The thermocouple was in direct contact with the catalyst, so that the thermocouple measurements could reflect the temperature inside the reactor. No temperature spike and temperature swings were observed during the whole catalytic testing at atmospheric pressure.

Carbon monoxide contained 5% nitrogen, which was used as an internal standard. Analysis of H_2, CO, CO_2, and CH_4 was performed with a 13X molecular-sieve column, while hydrocarbons (C1–C20) were separated in 10% CP-Sil5 on a Chromosorb WHP packed column. The selectivity of hydrocarbons was calculated on carbon basis. The FT reaction rate was expressed as a cobalt-time yield (in moles of converted CO per second divided by the total amount of cobalt (in moles) loaded into the reactor).

3. Results and discussion

3.1. Impregnated and calcined catalysts

The dried samples were investigated by UV–vis spectroscopy at room temperature and all exhibit the same absorption spectrum. The absorption bands at 511 and 1163 nm are characteristic of isolated mononuclear octahedral Co^{2+} species [18,19].

DTA/MS curves (not shown) show that in the absence of sorbitol, hexaaquacobalt(II) nitrate dehydrates into anhydrous $Co(NO_3)_2$

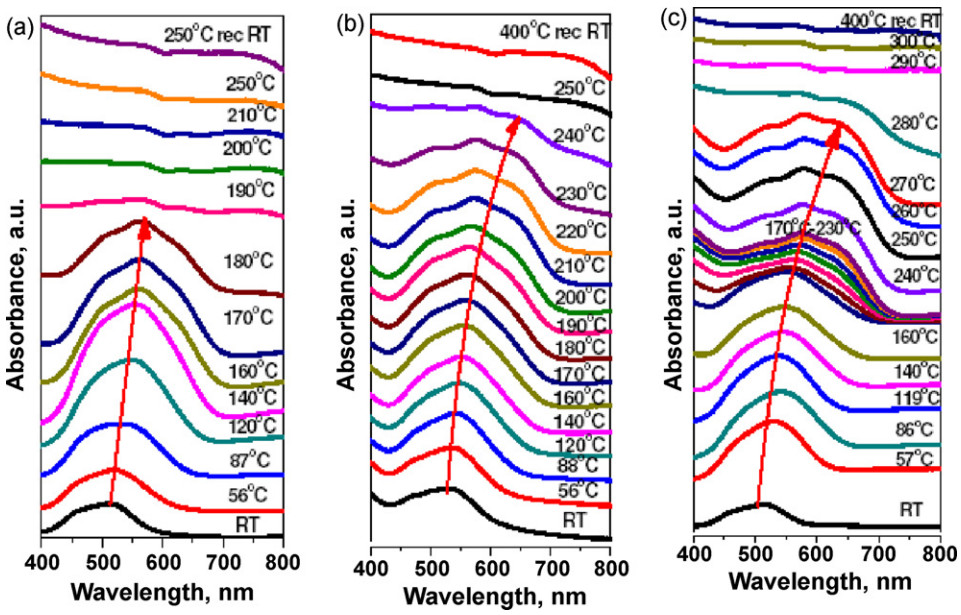

Fig. 1. In situ UV–vis spectra of (a) Co/SiO_2, (b) Co-Sorb(10)/SiO_2 and (c) Co-Sorb(2)/SiO_2 during calcination.

below 130 °C (H_2O (m/z 18)) and decomposes between 130 and 220 °C (NO (m/z 30), NO_2 (m/z 46)). When sorbitol is added, the decomposition of nitrates is divided into two steps: the first step takes place between 130 and 180 °C, as for the un-modified reference counterpart; the second step takes place together with the decomposition of sorbitol (CO_2 (m/z 44)), between 180 and 270 °C. Thus, sorbitol addition shifts the decomposition of cobalt nitrate to higher temperatures. Addition of sorbitol seems to result in an appearance of new cobalt species in the impregnated silica supported catalysts. These species decompose at higher temperatures than cobalt nitrate. Quantitative analysis of TGA/MS suggests that the weight loss peak located between 130 and 220 °C in the catalyst prepared without sorbitol corresponds to the decomposition of $Co(NO_3)_2$ into Co_3O_4. For the catalysts synthesized with sorbitol addition, the weight loss peak situated between 130 and 180 °C is assigned to the decomposition of cobalt nitrate species, and the peak at higher temperature is attributed to the decomposition reaction between cobalt nitrate and organic molecules, which occurs during partial oxidation of sorbitol (e.g. gluconic and saccharic acids) which can be produced during partial oxidation of sorbitol.

UV–vis spectra recorded in in situ conditions (Fig. 1) confirm these observations. With increasing temperature, the band corresponding to the $^4T_{1g}(F) \rightarrow {}^4T_{1g}(P)$ transition shifts towards the 570–580 nm region which is most probably because of dehydration of cobalt nitrate and a change of symmetry in the Co^{2+} environment (from octahedral to tetrahedral) [18]. The other detected change is the transformation of species containing ionic cobalt into Co_3O_4 (broad bands below 500 nm and above 600 nm). The more sorbitol is initially present on the catalyst, the higher is the temperature at which this transformation starts and completes. Sorbitol tends to stabilize ionic Co^{2+} before decomposition to Co_3O_4, probably by its coordination after cobalt nitrate dehydration.

X-ray absorption is a useful tool to monitor changes of cobalt phase in oxidation states [7,20]. Both XANES and EXAFS spectra were recorded in situ at the cobalt K edge every 500 ms. The spectra (Fig. 2a and b) show the transformation of cobalt phase from ionic Co^{2+} at room temperature into Co_3O_4 at elevated temperatures. The reference spectra of CoO and Co_3O_4 are also displayed in this figure. Interestingly, cobalt nitrate was directly converted into Co_3O_4, no intermediate cobalt compounds were detected using in situ

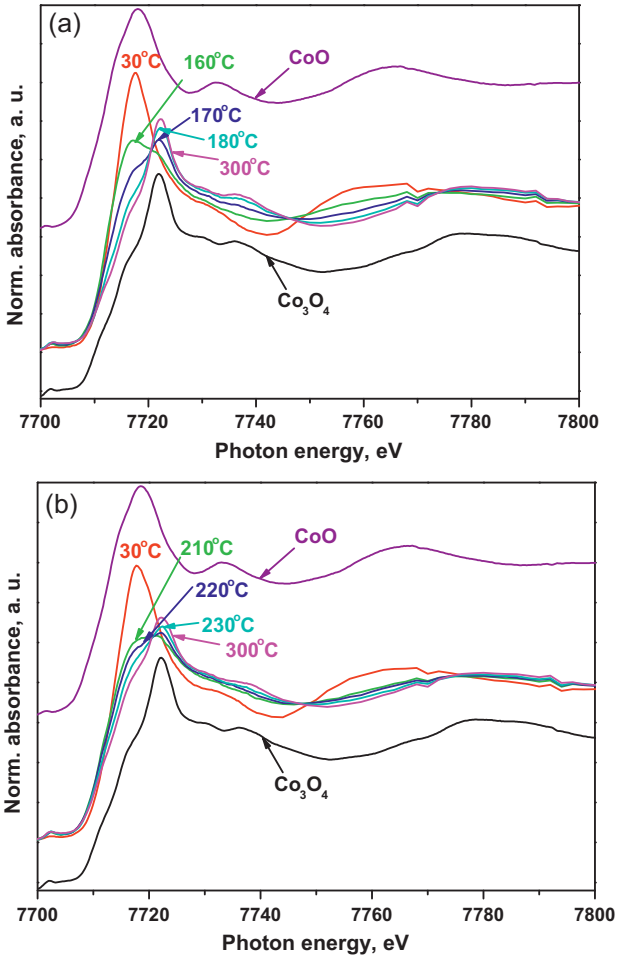

Fig. 2. In situ quick-XANES spectra of (a) Co/SiO_2 and (b) Co-Sorb(10)/SiO_2 during calcination.

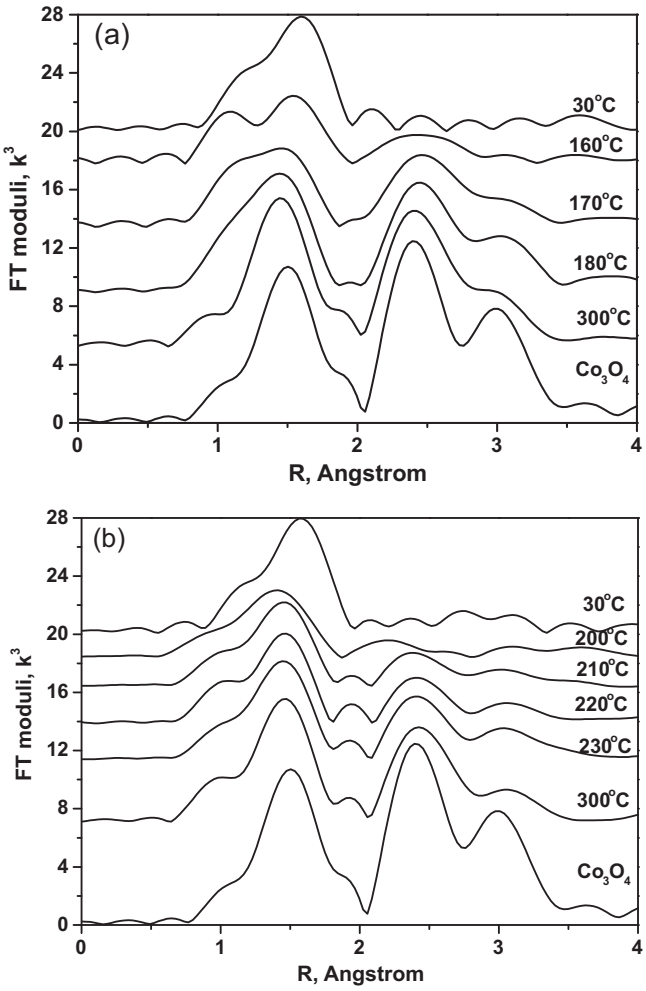

Fig. 3. Moduli of Quick-EXAFS Fourier transforms of (a) Co/SiO_2 and (b) Co-Sorb(10)/SiO_2 during calcination.

Quick-XAS even with high time resolution. Co_3O_4 formation starts from 170 °C in Co/SiO_2 catalyst, while in Co-Sorb(10)/SiO_2 catalyst, the formation of Co_3O_4 starts at 210 °C. Though temperature ranges are not exactly the same in UV–vis and XAS experiments, due to different configurations of the reactors, all results concur to show that sorbitol addition shifts the transformation to Co_3O_4 to higher temperatures (+40 °C). Previously [11] higher temperatures of decomposition of cobalt complexes and formation of Co_3O_4 were observed in silica-supported catalysts prepared with addition of sucrose.

The Fourier transform of the EXAFS signal is shown in Fig. 3, consistent with XANES. The second and third cobalt coordination shells of Co_3O_4 (~2.4 Å and 3.0 Å) in Co/SiO_2 appear from 170 °C, while these in Co-Sorb(10)/SiO_2 appear from 210 °C, 40 °C higher. Higher sorbitol content leads to higher temperature of cobalt nitrate complete decomposition.

The X-ray diffraction patterns of the four calcined cobalt-based catalysts are presented in Fig. 4. Co_3O_4 is the only cobalt-containing crystalline phase detected by XRD. Sorbitol addition results in a broadening of the diffraction peaks. After subtracting the contribution of the support, the average diameter of Co_3O_4 particles was assessed from the width of (3 1 1) and (4 4 0) diffraction peaks (Table 1). Both the diffraction reflections yield similar cobalt oxide crystallite sizes. The Co_3O_4 crystallite sizes in sorbitol-derived samples are much smaller than in the reference sample (4–6 nm compared with 10 nm) and a higher sorbitol content leads to

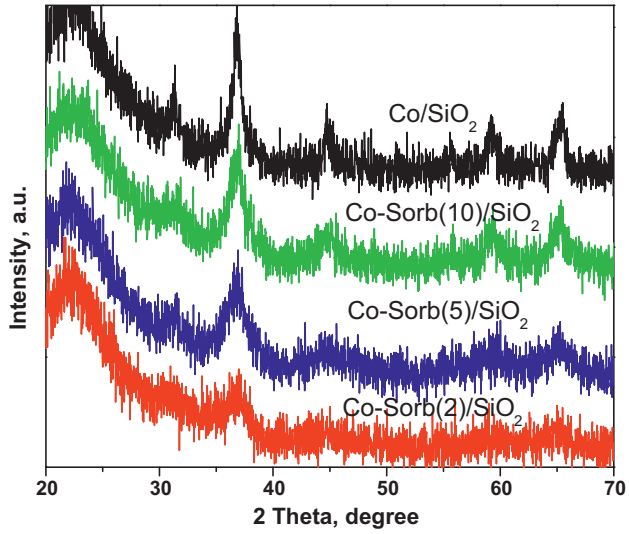

Fig. 4. XRD patterns of cobalt-based samples with different Co/sorbitol molar ratios, after calcination.

smaller crystalline domains. The suggestion about a smaller size of cobalt oxide particles in sorbitol-derived samples is consistent with EXAFS data. Indeed, the EXAFS Fourier transform moduli for second CoCo coordination shell indicate smaller coordination number in the calcined Co-Sorb/SiO_2 samples and thus smaller Co_3O_4 clusters.

3.2. Catalyst reducibility

The influence of sorbitol on the reducibility of supported cobalt catalysts was investigated both by temperature programmed reduction (TPR), in situ magnetic measurements and in situ Quick-X-ray absorption. In-situ Quick-X-ray absorption spectra (not shown) clearly show that Co_3O_4 reduction proceeds through the intermediate CoO. Both CoO and metallic cobalt were detected in the conventional catalyst prepared from cobalt nitrate after treatment with hydrogen at 500 °C, while mostly CoO species were identified from EXAFS in the sorbitol-derived sample. Several hydrogen consumption peaks are observed in the TPR profiles of the four catalysts (Fig. 5). The peaks below 180 °C could be attributed to the reductive decomposition of residual nitrate species [21,22]. The peaks between 200 and 450 °C are attributed to the two-step

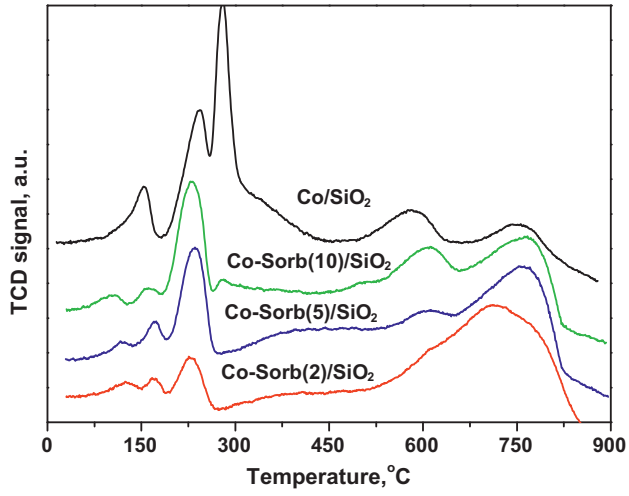

Fig. 5. TPR profiles of calcined cobalt-based samples with different Co/sorbitol molar ratios.

Table 2
FT catalytic performance of Co-based catalysts with different Co/sorbitol molar ratios.

Catal.	Conv. CO (%)	Sel. CH (%)					Co-time yield ($\times 10^{-4}$ s^{-1})	Adsorption propene (μmol/g-cat)
		CH_4	C2	C3	C4	C5+		
Co-Sorb(2)/SiO_2	3.2	16.1	2.6	7.8	9.7	63.8	1.4	18.5
Co-Sorb(5)/SiO_2	6.3	10.3	3.5	5.6	7.1	73.5	2.7	29.3
Co-Sorb(10)/SiO_2	3.8	9.8	4.5	5.4	7.1	73.2	1.6	18.7
Co/SiO_2	4.7	8.7	4.6	4.6	6.2	75.9	2.0	22.3

Reaction conditions: $m_{catal.}$ = 0.5 g, P = 1 bar, Temp. = 190 °C, GHSV = 1800 ml/g_{catal}/h, H_2/CO = 2.

reduction of Co_3O_4 particles to Co^0 via the intermediate CoO species [23,24]. The intensity of this peak decreases with increase in the amount of added sorbitol and with decrease in Co_3O_4 particle size, respectively. The second step (reduction of CoO into Co^0) is almost absent for the catalysts prepared using larger amounts of sorbitol. TPR peaks located at temperatures higher than 500 °C are assigned to the reduction of cobalt silicate-like species, which were not detected by X-ray absorption spectroscopy in the calcined samples. Previously it was shown [25] that such species could be formed by a reaction between smaller CoO particles and silica at higher temperatures in the presence of water produced during the TPR experiments. Consequently, the addition of sorbitol significantly decreases the size of cobalt oxide particles, but also hinders cobalt reducibility.

To better understand the reduction stages of these catalysts, in situ magnetic measurements were employed in this study (Fig. 6). It is known that the concentration of metallic cobalt phase can be selectively evaluated by monitoring the magnetization [15,16]. In situ magnetic results are qualitatively consistent with TPR findings and in situ Quick-XAS results. The presence of sorbitol resulted in a higher temperature of appearance of the metallic cobalt phase and magnetization was significantly lower in less reduced sorbitol-derived samples. Comparing the concentration of metallic cobalt phase after reduction in pure hydrogen at 400 °C, the investigated samples follow the order: Co/SiO_2 > Co-Sorb(10)/SiO_2 > Co-Sorb(5)/SiO_2 > Co-Sorb(2)/SiO_2. This ranking though cannot be directly correlated to the number of surface metallic sites exposed, since larger particles tend to be fully reduced but exhibit a low quantity of surface sites.

3.3. Catalytic performance

The catalytic performance of cobalt-based catalysts was evaluated in a differential catalytic reactor at 190 °C under atmosphere pressure. C_1–C_{20} hydrocarbons were the only reaction products under these conditions. The FT reaction rates are expressed as cobalt time yields, which are calculated from carbon monoxide conversion, inlet CO partial pressure, gas-space velocity and the amount of cobalt used for the reaction (Table 2).

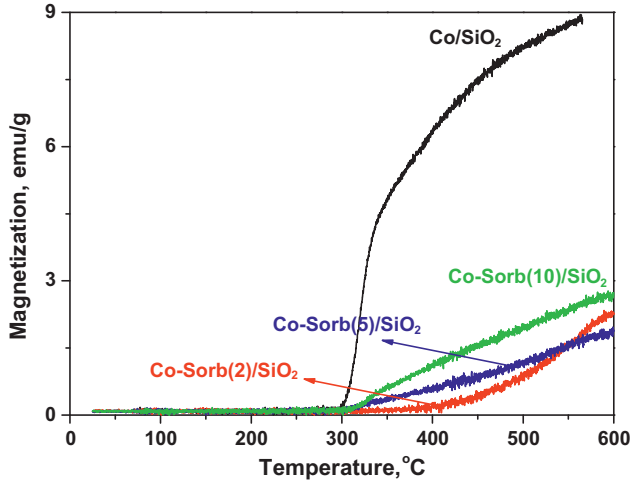

Fig. 6. In situ magnetization in pure hydrogen for calcined cobalt-based samples with different Co/sorbitol molar ratios.

The variations in terms of reaction rate are complex. The addition of a small amount of sorbitol (Co-Sorb(10)/SiO_2) lowers the reaction rate, but with the increase in sorbitol content, the catalytic activity passes through a maximum before decreasing again. Co-Sorb(5)/SiO_2 exhibits a slightly higher FT reaction rate (2.7×10^{-4} s^{-1}) than the reference catalyst (2.0×10^{-4} s^{-1}). One can also note a slight increase in CH_4 selectivity when sorbitol is used to prepare the catalysts.

The number of cobalt surface metal sites in the reduced catalysts was evaluated by propene chemisorption. It should be noted that propene chemisorption provides only relative information about the concentration of cobalt metal sites in different catalysts, since no assumption was made about the stoichiometry of this method [17]. The data in Table 2 indicate that the catalytic activity is proportional to the metallic surface area assessed by propene chemisorption. The cobalt-based catalysts investigated in this study thus present a very weak dependence of the FT turnover rate towards the cobalt particle size; the FT reaction rates normalized by propene chemisorption are nearly constant (~$13–15 \times 10^{-3}$ s^{-1}).

It is known that FT synthesis proceeds on cobalt metal sites, and the overall number of active sites on supported cobalt-based catalysts depends on both cobalt dispersion and reducibility [3]. We show here that cobalt oxide dispersion can be significantly enhanced by sorbitol addition in the impregnation solution. However, the smaller cobalt oxide particles are more difficult to reduce than larger Co_3O_4 crystallites in the reference catalyst. In addition, these small Co_3O_4 particles would form barely reducible cobalt silicate during thermal treatment in hydrogen flow. The number of cobalt metal sites and FT reaction rate appear to be a function of both cobalt particles size and cobalt reducibility with an optimum in the number of surface sites reached for Co-Sorb(5)/SiO_2. An efficient way to take advantage of sorbitol could be to increase the degree of cobalt reduction, through the addition of a reduction promoter to the catalyst, such as Pt or Ru.

4. Conclusion

The addition of sorbitol to the impregnation solution during the preparation of Co/SiO_2 catalysts has a strong impact on the one hand, on the size of Co_3O_4 particles on calcined catalysts, and on the other hand, on cobalt reducibility and FT catalytic performance. Sorbitol addition seems to stabilize supported Co^{2+} complexes. In the catalysts prepared with addition of sorbitol, cobalt complexes decompose at higher temperature. The decomposition of these complexes results in higher cobalt oxide dispersion. The higher is the content of sorbitol, the higher is the cobalt oxide dispersion.

The extent of cobalt reduction was lower in sorbitol-derived catalysts because of the presence of smaller and less reducible cobalt oxide particles. These smaller cobalt oxide particles can react with

silica during the reduction leading to cobalt silicate. The enhancement in cobalt dispersion and decrease in the degree of cobalt reduction produce antagonistic effects on the total number of cobalt sites active in the FT reaction, and thus on the overall catalytic activity.

Acknowledgements

The authors thank the French National Agency for Research (ANR, SAXO project) for financial support of this work. Soleil is acknowledged for the use of synchrotron radiation on beamline SAMBA.

References

[1] M.E. Dry, Catal. Today 71 (2002) 227–241.
[2] E. Iglesia, Appl. Catal. A 161 (1997) 59–78.
[3] A.Y. Khodakov, W. Chu, P. Fongarland, Chem. Rev. 107 (2007) 1692–1744.
[4] V.A. de la Pena O'Shea, N. Homs, J.L.G. Fierro, P. Ramírez de la Piscina, Catal. Today 114 (2006) 422–427.
[5] Z. Yan, D.B. Bukur, D.W. Goodman, Catal. Today 160 (2010) 39–43.
[6] A.K. Rausch, E. van Steen, F. Roessner, J. Catal. 253 (2008) 111–118.
[7] M. Rønning, N.E. Tsakoumis, A. Voronov, R.E. Johnsen, P. Norby, W. van Beek, Ø. Borg, E. Rytter, A. Holmen, Catal. Today 155 (2010) 289–295.
[8] C.C. Culross, US Patent 5 928 983 (1999).
[9] C.H. Mauldin, US Patent 5 968 991 (1999).
[10] C.H. Mauldin, US Patent 6 331 575 (2001).
[11] J.-S. Girardon, E. Quinet, A. Griboval-Constant, P.A. Chernavskii, A.Y. Khodakov, J. Catal. 248 (2007) 143–157.
[12] S. Sun, N. Tsubaki, K. Fujimoto, Appl. Catal. A 202 (2000) 121–131.
[13] B. Ravel, M. Newville, J. Synchrotron Radiat. 12 (2005) 537–541.
[14] B.D. Cullity, Elements of X-Ray Diffraction, Addison-Wesley Publishing Company, London, 1978.
[15] P.A. Chernavskii, A.Y. Khodakov, G.V. Pankina, J.-S. Girardon, E. Quinet, Appl. Catal. A 306 (2006) 108–119.
[16] P.A. Chernavskii, J.-A. Dalmon, N.S. Perov, A.Y. Khodakov, Oil Gas Sci. Technol. – Rev. IFP 64 (2009) 25–48.
[17] A.S. Lermontov, J.-S. Girardon, A. Griboval-Constant, S. Pietrzyk, A.Y. Khodakov, Catal. Lett. 101 (2005) 117–126.
[18] F. Dumond, E. Marceau, M. Che, J. Phys. Chem. C 111 (2007) 4780–4789.
[19] M. Mhamdi, E. Marceau, S. Khaddar-Zine, A. Ghorbel, M. Che, Y. Ben Taarit, F. Villain, Z. Phys. Chem. 219 (2005) 963–978.
[20] A.Y. Khodakov, J. Lynch, D. Bazin, B. Rebours, N. Zanier, B. Moisson, P. Chaumette, J. Catal. 168 (1997) 16–25.
[21] Ø. Borg, E.A. Blekkan, S. Eri, D. Akporiaye, B. Vigerust, E. Rytter, A. Holmen, Top. Catal. 45 (2007) 39–43.
[22] J. Hong, P.A. Chernavskii, A.Y. Khodakov, W. Chu, Catal. Today 140 (2009) 135–141.
[23] B. Ernst, A. Bensaddik, L. Hilaire, P. Chaumette, A. Kiennemann, Catal. Today 39 (1998) 329–341.
[24] D.G. Castner, P.R. Watson, I.Y. Chan, J. Phys. Chem. 94 (1990) 819–828.
[25] I. Puskas, T.H. Fleisch, P.R. Full, J.A. Kaduk, C.L. Marshall, B.L. Meyers, Appl. Catal. A 311 (2006) 146–154.